



HAL
open science

Comparing TiO₂ photocatalysis and UV-C radiation for inactivation and mutant formation of *Salmonella typhimurium* TA102

Antonino Fiorentino, Luigi Rizzo, H el ene Guilloteau, Xavier Bellanger, Christophe Merlin

► **To cite this version:**

Antonino Fiorentino, Luigi Rizzo, H el ene Guilloteau, Xavier Bellanger, Christophe Merlin. Comparing TiO₂ photocatalysis and UV-C radiation for inactivation and mutant formation of *Salmonella typhimurium* TA102. *Environmental Science and Pollution Research*, 2017, 24 (2), pp.1871 - 1879. 10.1007/s11356-016-7981-6 . hal-01767777

HAL Id: hal-01767777

<https://hal.univ-lorraine.fr/hal-01767777v1>

Submitted on 5 Oct 2021

HAL is a multi-disciplinary open access archive for the deposit and dissemination of scientific research documents, whether they are published or not. The documents may come from teaching and research institutions in France or abroad, or from public or private research centers.

L'archive ouverte pluridisciplinaire **HAL**, est destin ee au d ep ot et  a la diffusion de documents scientifiques de niveau recherche, publi es ou non,  emanant des  tablissements d'enseignement et de recherche fran ais ou  trangers, des laboratoires publics ou priv es.

14 **Abstract**

15 Salmonellosis is one of the most common causes of foodborne bacterial human disease worldwide and the
16 emergence of multidrug resistant (MDR) strains of *Salmonella enterica* serovar Typhimurium (*S.*
17 *typhimurium*) was associated to the incidence of invasive salmonellosis. The objective of the present work
18 was to investigate the effects of the TiO₂ photocatalysis process in terms of both bacteria inactivation and the
19 emergence of mutants, on *S. typhimurium* TA102 water suspensions. The TiO₂ photocatalysis was compared
20 with a conventional disinfection process *i.e.* UV-C radiation. In spite of the faster bacterial inactivation
21 obtained in UV-C disinfection experiments (45, 15 and 10 min for total inactivation for initial cell density 10⁹,
22 10⁸ and 10⁷ CFU mL⁻¹, respectively), photocatalytic disinfection (60, 30 and 15 min) was more energy efficient
23 because of a lower energy requirement (2 - 20 mWs cm⁻²) compared to the UV-C disinfection process (5 - 30
24 mWs cm⁻²). During the photocatalytic experiments, the mutation frequency increased up to 1648 fold
25 compared to background level for a 10⁸ CFU mL⁻¹ initial bacterial density, and mutants were inactivated after
26 1 - 10 min treatment, depending on initial bacterial cell density. In UV-C disinfection experiments, the
27 mutation frequency increased up to 2181 fold for a 10⁸ CFU mL⁻¹ initial bacterial cell density, and UV-C doses
28 in the range 0.5 - 4.8 mWs cm⁻² were necessary to decrease mutation frequency. In conclusion, both
29 disinfection processes were effective in the inactivation of *S. typhimurium* cells and mutants release into the
30 environment can be avoided if cells are effectively inactivated.

31

32 Keywords: advanced oxidation processes, Ames test, mutagenicity, *Salmonella typhimurium*, water
33 disinfection.

34

1. Introduction

36 Salmonellosis is one of the most common causes of foodborne bacterial human disease worldwide and a
37 significant increase in the number of *Salmonella* infections has been observed in many countries over the past
38 decade (Rahmani et al. 2013). Specifically, *Salmonella* spp. results in approximately 93.8 million cases of
39 gastroenteritis annually worldwide, leading to 155,000 deaths each year (Majowicz et al. 2010). The genus
40 *Salmonella* comprises two species *S. bongori* and *S. enterica*, the latter one being in turn divided in six sub-
41 species that cover more than 2550 serovars according to their O and H antigens. Among them, *S. enterica*
42 serovar Typhimurium, is a primary enteric pathogen mainly associated to human and other warm-blooded
43 vertebrates (Popoff 2001, Fàbrega and Vila 2013). In the last years, a close association was reported between
44 the emergence of multidrug resistant (MDR) strains of *Salmonella* and the incidence of invasive salmonellosis
45 (Gordon et al. 2008). The increased frequency of MDR *Salmonella* strains in human infections and the ensuing
46 consequences it has on a health perspective (Oubrim et al. 2012; Rahman et al. 2014), brings to light the
47 possible role of fecally contaminated waters in the spread of MDR *Salmonella* (Levantesi et al. 2012).

48 Food and water still play the main roles in the transmission of *Salmonella*. *Salmonellae* are excreted through
49 animal and human feces into the environment and are frequently found in aqueous matrices. In particular, they
50 typically occur in large numbers in raw sewage (Oubrim et al. 2012) and can still persist in wastewater
51 effluents (Masarikova et al. 2016) even after a disinfection process (Wéry et al. 2008). A study indicated that
52 80% of wastewater samples used for irrigation was positive for *Salmonella* (Nutt et al. 2003). Moreover, it
53 has been detected in various types of natural waters such as rivers, lakes, coastal waters, as well as
54 contaminated ground water (Polo et al. 1999; Martinez-Urtaza et al. 2004; Haley et al. 2009; Levantesi et al.
55 2010).

56 Different studies have investigated the inactivation of *Salmonella* strains by disinfection processes in water
57 and wastewater. In particular, Koivunen and Heinonen-Tanski (2005) evaluated the effect of different
58 disinfection processes on *Salmonella* strains in synthetic wastewater where the treatment with peracetic acid
59 and UV radiation has been shown to be faster than UV radiation alone and chlorine processes for the
60 inactivation of *Salmonella enteritidis*. In some instance, *Salmonella* has been found to be more resistant to
61 disinfection processes than others bacterial indicators (Berney et al. 2006; Rincon and Pulgarin 2007, Sciacca
62 et al. 2011; Li et al. 2012). On the other hand, conventional disinfection by either chlorination or UV radiation
63 may not be effective enough in controlling the spread of pathogens including ~~resistant microorganisms and~~

64 particularly antibiotic resistance microorganisms (Rizzo et al. 2013), therefore alternative disinfection
65 methods should be investigated. Advanced oxidation processes (AOPs) (e.g., Fenton, photo-Fenton, TiO₂
66 photocatalysis, UV/O₃, UV/H₂O₂ etc.) have been found effective in the removal of a wide range of
67 contaminants (Rizzo 2011). Among AOPs, TiO₂ photocatalysis is a promising water disinfection option,
68 because of its capacity to inactivate a wide range of pathogens in water (Dunlop et al. 2011; Polo-López et al.
69 2014; Rizzo et al. 2014a); however, to the best of our knowledge, the effectiveness of TiO₂ photocatalysis on
70 the inactivation of selected *Salmonella* strains and/or its possible effect in terms of mutagenicity has not been
71 investigated so far. Indeed, if the inactivation of microbial indicators during treatment/disinfection processes
72 is well documented, specific process-induced mutagenicity is generally occulted, apart from demonstrating
73 the production of genotoxic by-products. Yet, in *Salmonella* as for other organisms, gene mutations can confer
74 resistance to antimicrobial by altering the corresponding protein target or by altering the substrate specificity
75 of existing antimicrobial degrading enzymes (Michael et al. 2006). Thus, beyond bacterial inactivation,
76 considering process-induced mutagenicity might prove to be of prime importance for a better control of
77 antibiotic resistance pathogens in the released effluents. In fact, antibiotic resistances can be acquired either
78 through gene transfer or by mutation of the target gene. If the effects of various treatment strategies on the
79 persistence of resistance genes/bacteria start now to be relatively well documented, the effects of such
80 treatments on the emergence (mutation) and dissemination (transfer) of antibiotic resistance genes remains
81 scarce nay inexistent, and needs further consideration (Sharma et al 2016).

82 The objective of the present work was to investigate the effects of the TiO₂ photocatalysis process in terms of
83 inactivation and mutagenicity on a model microorganism. *Salmonella* was chosen as target/model organism
84 (its genus belongs to the *Enterobacteriaceae*, the same family as *Escherichia*, which includes the species *E.*
85 *coli*) because of (i) its spread in aqueous matrices (particularly in natural water and wastewater), (ii) the related
86 concern for human health (it can cause illnesses such as typhoid fever and paratyphoid fever) and (iii) its role
87 in antibiotic resistance spread. Moreover, the effect of TiO₂ photocatalysis on the inactivation and
88 mutagenicity of *Salmonella* was compared with a conventional disinfection process *i.e.* UV-C disinfection.

89 **2. Material and methods**

90 **2.1 Bacterial strain and media**

91 *Salmonella enterica* serovar Typhimurium strain TA102 was used as tester strain for general mutagenicity
92 testing according to Maron and Ames (1983). Strain TA102 has been extensively used and reported under its
93 former species name “*Salmonella typhimurium*” and will be reported as such in this manuscript to avoid
94 unnecessary confusion. Strain TA102 exhibits a requirement for histidine and therefore cannot grow on
95 minimal medium unless the *his428* mutation, carried on its plasmid pAQ1, mutates back to a prototrophic
96 form. *S. typhimurium* TA102 was routinely cultured at 37°C on Vogel-Bonner minimal medium supplemented
97 with D-Glucose, D-Biotin and L-Histidine (Maron and Ames 1983). For isolation of His⁺ revertants, the
98 histidine supplement was omitted from the medium. Strain *S. typhimurium* TA102 was selected among a
99 variety of other *Salmonella* tester strains because of its noticeable sensitivity to numerous mutagenic agents,
100 including UV, that are otherwise poorly detected by alternative tester strains (Maron and Ames 1983).
101 TA102 bacteria were unfrozen and revived by streaking on Vogel-Bonner agar plate supplemented with
102 Glucose and Histidine and incubated at 37 °C for 48 h. A single colony from the plate was inoculated into 10
103 mL sterile lysogeny broth (LB, Sigma-Aldrich, USA) and incubated at 30°C for 18 h under agitation (160
104 rpm) in a rotating shaker to obtain a stationary phase culture. Cells were washed twice by alternating
105 centrifugations at 5000 rpm for 2 min and pellets re-suspensions in 10 mM MgSO₄. The final volumes were
106 adjusted to obtain cell concentrations at either 10⁹, 10⁸ or 10⁷ CFU mL⁻¹; these suspensions were prepared
107 independently and then used in independent disinfection experiments.

108

109 **2.2 TiO₂ photocatalysis tests**

110 Photocatalytic tests were carried out in a 2.2 L cylindrical glass reactor (13.0 cm in diameter) filled in with
111 the 400 mL of sample. The thickness of liquid was constant and equal to the liquid depth (3 cm). The reactor
112 was placed in a water bath to control the temperature at 30°C during the experiments. The aqueous suspension
113 in the reactor was stirred continuously. A wide spectrum 250 W lamp (Procomat, Italy) with a peak of light
114 intensity in the UV-A range of 0.012 mW cm⁻² at 350 nm was used as light source. The lamp was placed
115 horizontally, 40 cm above the surface of the water. Degussa P25 TiO₂ was used as slurry as received from the
116 manufacturer to perform heterogeneous photocatalytic experiments. They were carried out at concentration of
117 100 mg L⁻¹ according to previously set conditions (Rizzo et al. 2014b). Finally, control tests with TiO₂ under
118 dark conditions and UV irradiation alone were carried out in order to distinguish their respective contribution

119 to *S. typhimurium* TA102 inactivation and stress-induced mutagenicity compared to the photocatalytic
120 process.

121

122 **2.3 UV-C disinfection tests**

123 UV-C experiments were carried out in 40 mL glass Petri dishes (diameter: 90 mm) filled in with 25 mL of
124 sample. Petri dishes were gently stirred throughout the exposure time under a collimating apparatus (Simonet
125 and Gantzer, 2006) equipped with a low-pressure mercury vapor lamp (10-W Slimline germicidal lamp,
126 ozone-free Ster-L-Ray G12T6L; Atlantic UV Corporation) emitting monochromatic (253.7-nm) UV light.
127 The irradiance at the center of the beam at the water surface was about 0.008 mW cm⁻², and was delivered by
128 a UV tube positioned horizontally, 20 cm above the surface of the water. Different UV-C doses were achieved
129 by varying the exposure time

130

131 **2.4 Bacterial count and mutation frequencies**

132 Bacterial cells exposed to UV-C and TiO₂ photocatalysis treatment were recovered, serially diluted in 10 mM
133 MgSO₄, and spread in triplicate on minimal glucose agar with and without histidine. Plates were incubated at
134 37°C for 48-72h. Each sample was analyzed in triplicate. Mutation frequencies were obtained as ratios
135 between the number of revertants (counts on plates without histidine) and the total bacterial cell counts (on
136 medium with histidine).

137

138 **2.5 Statistical analysis**

139 The correlations between the bacterial mortality ($\log(N/N_0)$) and the duration of the treatments, or the doses
140 received, were assessed using the Pearson's test. Then, regression data analyses were performed on log-
141 transformed data: $\log(N/N_0)$ for the total cell counts and $\log(F/F_0)$ for the frequencies of mutation. The effects
142 of both the treatment and the initial bacterial cell load were analyzed using a Fisher F-test and a Student T-
143 test. The "Fisher F-test" was used to test data for homogeneity of variances. Thereafter, once homogeneity
144 was verified, a "Student T-test" was further used to compare the trends (slopes) of linear regressions. A
145 statistical difference revealed by a Student T-test, combined to the comparison of regression trendlines (slopes)

146 allowed determining whether a given treatment or condition had stronger effects than another one. Statistical
147 correlations and statistical comparisons are presented in supplementary material.

148

149 **3. Results and discussion**

150 **3.1 TiO₂ photocatalytic tests**

151 *3.1.1 Control tests*

152 Photocatalytic tests were carried out by using a wide spectrum lamp with the main emission in UV-A
153 wavelength range (400-315 nm) and TiO₂ as photocatalyst. Therefore, control tests were carried out using
154 UV-A radiation and TiO₂ as stand-alone processes in order to evaluate the effective contribution of
155 photocatalytic process (UV/TiO₂) on both the inactivation of strain TA102 and the induction of His⁺ revertant
156 mutants.

157 TiO₂ control experiments were carried out in the dark and did not result in any significant change neither in
158 the initial bacterial density and nor the mutants count (2h treatment; data not shown). UV-A control tests were
159 carried out up over time to 15, 30 and 60 min irradiation time with initial cell suspension density of 10⁷, 10⁸
160 and 10⁹ CFU mL⁻¹, respectively, according to the respective minimum treatment time necessary to achieve
161 total *S. typhimurium* TA102 inactivation by the corresponding UV/TiO₂ process. As shown in Figure 1 and
162 Supplementary section 3, the UV-A control tests resulted in a moderate (but statistically significant) cell
163 inactivation and weak changes in mutation frequency over the course of the UV-A exposure time

164

165

Figure 1

166

167 The bacteria inactivation clearly appears exposure time dependent, it did not seem to be significantly
168 influenced by initial cell load as for a given time of UV-A exposure a similar cell count reduction is observed
169 (ca. 1 log reduction for a 15 min exposure). On a statistical point of view, the decreasing trend in viable cell
170 counts correlates with the exposure time but the absence of homogenous variances does not allow drawing
171 any conclusion regarding a possible effects of the initial cell load (Supplementary sections 2 and 3). The
172 evolution of the His⁺ mutant counts appear to decrease at a slower pace compared to the total viable count,
173 with 0.5 log units decrease after 15 min to 2.2 log units decrease after 60 min treatment time (Figure 1a). This

174 may indicate that an increase of the mutation frequency, therefore producing more His⁺ mutants, could
175 partially compensate the inactivation of the His⁺ subpopulation. This seems to be particularly true for the 10⁹
176 CFU mL⁻¹ initial cell density suspension, where a 231 fold increase of the mutation frequency was reached
177 after 60 min of UV-A exposure. Nevertheless, when comparing the different evolution of the mutation
178 frequencies (log F/F₀) as a function of the treatment dose (exposure time), no statistical difference was
179 observed between the different initial cell loads (Supplementary Fig. S2, Table S3).

180 The inactivation of *S. typhimurium* TA102 can be explained through the damage caused by UV-A radiation
181 following its absorption by cellular components called intracellular chromophores. Light absorption through
182 chromophores contributes to the generation of reactive oxygen species (ROS). According to McGuigan et al.
183 (2012), the UV-A wavelengths bordering on visible light are not sufficiently energetic to alter DNA directly.
184 Nevertheless, UV-A play an important role in promoting the formation of intracellular ROS (singlet oxygen,
185 superoxide, hydrogen peroxide, and hydroxyl radical), which can in turn damage DNA.

186

187 3.1.2 *S. typhimurium* TA102 inactivation by TiO₂ photocatalysis

188 The results of *S. typhimurium* TA102 inactivation by TiO₂ photocatalysis are plotted as function of irradiation
189 time in Figure 2.

190

191 Figure 2

192

193 The initial bacterial density strongly affected the inactivation rate by TiO₂ photocatalysis (Fig. 2;
194 Supplementary section 4). The complete bacterial inactivation was achieved after 60, 30 and 15 min of
195 irradiation for initial bacterial densities of 10⁹, 10⁸ and 10⁷ CFU mL⁻¹, respectively. Compared to control test
196 with UV-A radiation alone (Fig.1), TiO₂ photocatalytic process was found to be undoubtedly more effective,
197 which was further demonstrated by a Student comparison T-tests on both series of data (Supplementary section
198 6). Cho et al. (2004) evaluated the correlation between hydroxyl radicals ([•]OH) and *E. coli* inactivation rates
199 under UV/TiO₂ treatment. The concentration of [•]OH during photocatalytic treatment was quantified by
200 measuring p-chlorobenzoic acid (a probe compound) degradation rate. The results demonstrated an excellent
201 linear correlation between [•]OH and the rate of *E. coli* inactivation, which indicates that the [•]OH radical is the
202 primary oxidant species responsible for inactivating *E. coli* in the UV/TiO₂ process. The inactivation of *S.*
203 *typhimurium* TA102 by photocatalysis with UV-A lamp in combination with TiO₂ at concentration of 0.5 g L⁻¹

204 ¹ was studied by Long et al. (2014). Three different initial cell loads were investigated: 10^7 , 10^6 and 10^5 CFU
205 mL^{-1} , and a complete inactivation was reached after 180, 70 and 60 min respectively. Slower inactivation rates,
206 as might be expected, were obtained with only the UV-A lamp. A similar study, with the inactivation of
207 *Salmonella enteritidis* (initial bacterial density of 10^8 CFU mL^{-1}) by UV-A lamp and TiO_2 at concentration of
208 1.0 g L^{-1} was carried out by Robertson et al. (2005). A decrease of 5 log units was reached after 120 min of
209 treatment, however, quite surprisingly, little difference was observed in experiments without catalyst and only
210 with UV-A lamp. In our previous experiments, the effect of TiO_2 /sunlight experiment on antibiotic resistant
211 *Escherichia coli* strains was investigated by using the same experimental set up (2.2 L cylindrical glass reactor
212 and 250 W lamp) and a total inactivation was achieved after 60 min, with 100 mg L^{-1} of TiO_2 and an initial
213 bacterial load of 10^6 CFU mL^{-1} (Rizzo et al. 2014b). Wang et al. (2014) also reported that the rate of bacterial
214 inactivation, or real antimicrobial activity by TiO_2 , depends on the initial bacterial concentration. In the present
215 study, we also found that the inactivation rate of strain TA102 was exposure time-dependent and statistically
216 stronger as the initial cell load decrease (Supplementary section 4). Possibly, when the initial bacteria
217 population is too high, there is a bigger buffering capacity for the hydroxyl radicals, which is not only due to
218 the large amount of cells but also from the mineralization products in the reaction process. In 2011, Foster et
219 al. proposed a killing mechanism where hydroxyl radicals progressively damage the cell surface structures
220 leading to the release of intracellular material/molecules that can in turn be undergo further degradation up to
221 a complete mineralization. From this it can then be assumed that the released intracellular components here
222 seen as intermediate products of photocatalysis, have a protective effect on live bacteria as they compete with
223 live cells for interacting with hydroxyl radicals, and thus contribute to the loss of antibacterial activity. ~~In our~~
224 ~~previous experiments, the effect of TiO_2 /sunlight experiment on antibiotic resistant *Escherichia coli* strains~~
225 ~~was investigated by using the same experimental set up (2.2 L cylindrical glass reactor and 250 W lamp) and~~
226 ~~a total inactivation was achieved after 60 min, with 100 mg L^{-1} of TiO_2 and an initial bacterial load of 10^6 CFU~~
227 ~~mL^{-1} (Rizzo et al. 2014b).~~

228 In spite of the debate over which process lead to death of an organism exposed to photocatalytic action, most
229 of the experimental evidences show that the destruction of the cell membrane is an important issue for
230 inactivation (Dalrymple et al. 2010). The mechanism for bacterial destruction by TiO_2 photocatalysis has been
231 proposed to occur via attack by $\cdot\text{OH}$ generated on the photocatalyst surface and the mode of microbial
232 destruction suggest that initial target for photocatalytic attack is the bacterial cell wall. Gram-negative cell
233 wall includes a thin peptidoglycan layer, and an external membrane made of lipopolysaccharide (LPS) and

234 phospholipid. In gram-negative bacteria, peptidoglycan layer makes up only about 10% of the cell wall and it
235 is likely that it may be susceptible to radical attack (Lu et al. 2003). LPS layer and the phospholipid bilayer
236 are made up of fatty acids, which may be also susceptible to radicals attack. The possibility of radicals to travel
237 only very short distances and the presence of an intact membrane reduce the probability of the radical reaching
238 intracellular components such as DNA, but once the radicals are generated in close proximity to the target
239 molecules, they will be able to inflict injury directly (Dalrymple et al. 2010). On the other hand, two $\cdot\text{OH}$
240 radicals may recombine to form hydrogen peroxide, which may inactivate bacterial cells on a longer distance
241 between the source of radicals and the target (Foster et al. 2011).

242

243 3.1.3 *S. typhimurium* mutagenicity during TiO_2 photocatalysis tests

244 The mutation frequencies were also evaluated following the TiO_2 photocatalytic tests, and displayed a 42,
245 1648, 32 fold increase compared to background level for a 10^9 , 10^8 and 10^7 CFU mL^{-1} initial bacterial density,
246 respectively (Fig. 2). The evolution of the mutation frequencies as a function of the treatment exposure time
247 displayed biphasic aspects with an initial increase followed by a slow-down or a decrease as the exposure time
248 increases. It is worth noting that the increased mutation frequencies are not associated to dramatic increases
249 of the mutants counts; considering the fact that the emerging mutants are also subjected to an increase loss of
250 cell viability, the apparent stability of the mutants counts probably result from an increased mutation frequency
251 counterbalanced by an increased cell killing. If the levels of mutation reached were clearly different depending
252 on the initial cell load (Fig. 2), statistical analyses demonstrated that the evolution of the mutation frequency
253 (as a function of the exposure time) were similar for the 10^8 and 10^7 CFU mL^{-1} initial cell load (Supplementary
254 section 4). This tends to show (i) that the treatment is in fact equally effective for these two initial cell loads
255 in terms of dose-dependent effects, but (ii) the 10^7 CFU mL^{-1} suspension stops accumulating mutations earlier
256 than the 10^8 CFU mL^{-1} probably because of a stronger killing effect.

257 The effect of different oxidants/disinfectants (namely chlorine, chlorine dioxide and ozone) on genotoxicity
258 has been studied by different authors (Monarca et al. 2000; Mišić et al. 2011; Magdeburg et al. 2014), but no
259 information is available in scientific literature (to authors' knowledge) on the effect of photocatalytic processes
260 on the induction of mutants in *Salmonella* strains after treatment. Basically, *Salmonella* disinfection-induced
261 mutagenicity has been mainly related to the formation of disinfection by-products. For example, Magdeburg
262 et al. (2014) studied the effect of ozone, as tertiary treatment, in a pilot scale wastewater treatment. The Ames
263 assay using *Salmonella typhimurium* strain YG7108 revealed an ozone-dose dependent mutagenicity increase

264 after wastewater ozonation, indicating the formation of alkylating mutagenic oxidation by-products. The
265 impact of ozone treatment on genotoxic and acute toxic effects of tertiary treated municipal wastewater was
266 investigated by Mišík et al. (2011). After ozone treatment, they observed a decrease of the mutagenic activity
267 of the samples and the bactericidal effects were reduced by ozonation. The influence of disinfectants such as
268 chlorine dioxide, ozone, peracetic acid and, UV radiation, on the formation of mutagenic compounds has been
269 evaluated by Monarca et al. (2000). They evaluated the mutagenicity using the Ames test and all disinfectant
270 treatments induced the formation of mutagenic compounds, particularly chemical treatment with ClO₂ or
271 ozone, in contrast with physical treatment with UV-C lamp.

272 Despite the lack of work available in scientific literature concerning the effect of TiO₂ photocatalytic process
273 on the formation of mutants in *Salmonella* strains, the possible role of hydroxyl radicals has been investigated
274 (Kanno et al. 2012). De Kok et al. (1992) used electron spin resonance (ESR) spectroscopy to detect and
275 identify oxygen species generated by fecapentaenes (potent genotoxins found in human feces) and investigated
276 the influence of scavenging reactive oxygen species (dimethyl sulfoxide (DMSO), t-butyl alcohol, t-butyl
277 hydroperoxide (TBOOH), 2,2,6,6-tetramethylpiperidine and 5,5-dimethyl-1-pyrroline-A'-oxide) on the
278 mutagenicity of *Salmonella* strains including TA102. All hydroxyl radical scavengers significantly reduced
279 the number of revertants (except for DMSO in combination with TBOOH), thus showing that hydroxyl radical
280 could mediate mutagenicity of the *Salmonella* strains although the precise mechanisms did not appear clearly
281 identified. In another study, hydrogen peroxide-induced mutagenicity in *Salmonella typhimurium* TA102 was
282 assumed to be caused by hydroxyl radicals generated by iron ions closely associated with DNA, since iron
283 chelators or hydroxyl radical scavengers (ascorbic acid or DMSO) exhibited effective anti-mutagenic effects
284 (Grey and Adlercreutz, 2003).

285

286 **3.2 UV-C disinfection tests**

287 *3.2.1 S. typhimurium TA102 inactivation by UV-C disinfection tests*

288 UV-C irradiation tests were carried out in order to compare the results from TiO₂ photocatalytic process with
289 a more conventional disinfection process. Figure 3 shows the evolution of cell counts and mutation frequencies
290 as a function of UV energy. Control tests carried out in the dark (sample stored at room temperature for 4
291 hours) did not show any change in bacterial cultivability (data not shown).

292

Figure 3

293

294

295 Whatever the initial cell load, a progressive loss of cultivability of strain TA102 was observed as the UV-dose
296 was increased, which was confirmed by a Pearson correlation test (Supplementary section 2). For the highest
297 initial cell load (10^9 CFU mL⁻¹), the total cell count dropped down by 9 log units and total inactivation was
298 reached after about 45 min of UV exposure (Fig.3a), which correspond to a 30 mWs cm⁻² (45 min irradiation
299 time) UV-C dose. As the initial bacterial density was decreased to 10^8 (Fig. 3b) and 10^7 (Fig. 3c) CFU mL⁻¹,
300 the total bacteria inactivation was achieved in 15 and 10 min, respectively while the corresponding UV-C
301 doses were relatively close in both experiments (approximately 5-10 mWs cm⁻²). Statistically, the cell count
302 abatements ($\log(N/N_0)$) appeared similar in terms of dose-dependent decrease for the two lower initial cell
303 loads (Supplementary section 5) although longer treatment are necessary to achieve a full inactivation of the
304 higher initial cell load. The cell count abatement obtained for the 10^9 CFU mL⁻¹ suspension appeared to
305 decrease at a significant lower pace (Supplementary Fig. S5) compare the two other suspensions, which
306 probably reflect the shield effect exerted by bacteria when the cell density is too high. However, a direct
307 dependence of initial concentration of microorganism and UV dose necessary to reach a full cell inactivation
308 was expected. Its estimation was based on the averaged incident radiation energy over the reactor volume that
309 is a dynamic function of the absorption coefficient, which itself depends dynamically on the concentration of
310 active cells (Silva et al. 2013). UV-C disinfection relies on the sensitivity of the microorganism to UV
311 radiation. This is unique to each microorganism and is determined by its ability to absorb at 200–280 nm
312 (germicidal wavelength range), so inactivating their active cells through UV-induced damages such as the
313 formation of pyrimidine dimers in their DNA. UV-induced damages disrupt the DNA structure, so that, if a
314 critical number of dimers is formed, the DNA cannot replicate (Hignen et al. 2006).

315 At a first glimpse, the cell complete inactivation was faster in the UV-C disinfection experiments compared
316 to photocatalytic disinfection experiments for all initial bacterial densities investigated (Fig.2). However,
317 considering the energy engaged in both treatments, the photocatalytic process was more efficient than the UV-
318 C process because a lower energy was required to achieve a total *S. typhimurium* inactivation (in the range 2
319 - 20 mWs cm⁻²).

320

321 3.2.2 *S. typhimurium* mutagenicity during UV-C disinfection tests

322 The mutation frequencies, increased in a UV-C dose dependent manner to reach a maximum corresponding
323 to a 21, 2181 and 26 fold increase compared to background level, for 10^9 , 10^8 and 10^7 CFU mL⁻¹ initial
324 bacterial density, respectively (Fig. 3). UV-C doses higher than 7.2, 2.4 and 0.5 mWs cm⁻² respectively,
325 resulted in absence of detectable mutants, where the deleterious effect of the UV-C treatment ultimately
326 dominates over the emergence of mutants (Fig.3). As for the photocatalytic treatment, the evolution of the
327 mutation frequencies displayed a dose-dependent biphasic aspects with an initial increase followed by a slow-
328 down/decrease for higher UV-C doses. Here again, statistical analysis demonstrated that the initial increase of
329 the log(F/F₀) ratio appeared to evolve at a lower pace for the 10^9 CFU mL⁻¹ cell suspension than the 10^8 and
330 the 10^7 CFU mL⁻¹ ones (Supplementary section 5), which mean that different initial cell load are not equally
331 sensitive as far as cell are numerous enough to exert a shield effect. UV radiation produces many types of
332 photochemical alterations (e.g., in DNA, RNA, protein, membranes) but DNA remains the major target for
333 the deleterious effects of UV radiation all together because of its large size, its efficient UV absorption, its
334 low number of copies per cells, and finally because it is the support of genetic information (Grossweiner et al.
335 2005). A large number of different types of damage are produced in DNA by UV irradiation however,
336 mutagenic lesions principally result from the formation of pyrimidine dimers and pyrimidine adducts (Sinha
337 and Häder 2002). UV-induced mutagenesis is a highly complex process involving different photoproducts and
338 repair mechanisms that deal with them. Tate et al. (2006) characterized the damage of UV-C radiation in
339 *Salmonella typhimurim* strain TA98. The damage was found primarily localized in the nucleic acids and it
340 results from direct absorption of photons by the target molecules. According to the authors, the damage
341 produced by UV-C was predominately in the form of pyrimidine dimers and 6-4 photoproducts resulting from
342 the direct photon absorption by DNA. UV-induced mutations in *Salmonella* are relevant not only regarding
343 lethality, but also because it may favor the appearance of some antibiotic resistances (Michael et al. 2006).
344 With this respect, it is worth noting that in the case of UV-C disinfection tests carried out with 10^7 CFU mL⁻¹,
345 a one log increased titer of His⁺ mutants was observed together with the increasing mutation frequency.
346 Possibly in this setup, from 0 to 0.2 mWs cm⁻², the appearance of mutants is not compensated by cell death as
347 the mutation frequency increases. This was also observed but to a lesser extent with the other treatment.

348

349 4. Conclusions

350 TiO₂ photocatalysis was compared with UV-A (control) and UV-C radiations both in terms of cell inactivation
351 and appearance of mutants in *Salmonella typhimurium* TA102 dispersed in water. In the investigated
352 conditions, the inactivation rate appeared faster in the UV-C radiation experiments (10 min for total
353 inactivation with an initial density of 10⁷ CFU mL⁻¹) than the photocatalytic experiments (15 min). But
354 photocatalytic process was more energy efficient because a lower energy was required (2 - 20 mWs cm⁻²,
355 depending on initial bacterial density) compared to UV-C disinfection process (5 - 30 mWs cm⁻²). In most
356 experiments, the appearance of mutants seemed to be counterbalanced by cell death, which results in an
357 increasing mutation frequency with no increase of the His⁺ mutant titers. In some case though, a significant
358 increase of the His⁺ mutant titers was observed before full inactivation. Possibly, in particular conditions
359 where disinfection is incomplete, the selected process may pose a risk of releasing more mutants than untreated
360 cell suspensions, with possible consequences regarding mutation-dependent acquisition of antibiotic
361 resistances. Statistically, both the bacterial inactivation and the evolution of the mutation frequencies appeared
362 directly dependent of initial concentration of microorganism and treatment dose, whatever the treatment, UV-
363 C or photocatalysis respectively. This necessarily implies to carefully consider the cell density if the generation
364 of mutants is to be prevented in disinfection setup.

365

366

367 Acknowledgements

368 The support of University of Salerno through FARB2012 (Trattamento avanzato di acque reflue urbane
369 mediante fotocatalisi: effetto sui batteri resistenti agli antibiotici) project funding is acknowledged. The
370 authors would like also to acknowledge the financial support provided by COST-European Cooperation in
371 Science and Technology, to the COST Action “TD0803: Detecting evolutionary hotspots of antibiotic
372 resistances in Europe (DARE)” and COST Action “ES1403: New and emerging challenges and opportunities
373 in wastewater reuse (NEREUS)”. CM wishes to thank the “Zone Atelier Moselle” (ZAM) for supporting his
374 research on treatment processes and their effects. Disclaimer: The content of this article is the authors’

375 responsibility and neither COST nor any person acting on its behalf is responsible for the use, which might be
376 made of the information contained in it.
377
378

379 **References**

- 380 Berney HU, Weilenmann A, Simonetti T (2006) Efficacy of solar disinfection of *Escherichia coli*,
381 *Shigella flexneri*, *Salmonella* Typhimurium and *Vibrio cholerae*. J Appl Microbiol 101(4):828-836
- 382 Cho M, Chung H, Choi W, Yoon J, (2004) Linear correlation between inactivation of *E. coli* and OH
383 radical concentration in TiO₂ photocatalytic disinfection. Water Res 38:1069–1077
- 384 Dalrymple OK, Stefanakos E, Trotz MA, Goswami DY (2010) A review of the mechanisms and
385 modeling of photocatalytic disinfection. Appl Catalysis B: Environ 98:27–38
- 386 de Kok TM, van Maanen JM, Lankelma J, ten Hoor F, Kleinjans JC (1992) Electron spin resonance
387 spectroscopy of oxygen radicals generated by synthetic fecapentaene-12 and reduction of fecapentaene
388 mutagenicity to *Salmonella typhimurium* by hydroxyl radical scavenging. Carcinogenesis 13:1249–
389 1255
- 390 Dunlop PSM, Ciavola M, Rizzo L, Byrne JA (2011) Inactivation and injury assessment of *Escherichia*
391 *coli* during solar and photocatalytic disinfection in LDPE bags. Chemosphere 85:1160-1166
- 392 Fàbrega A, Vila J (2013) *Salmonella enterica* serovar Typhimurium skills to succeed in the host:
393 virulence and regulation. Clin Microbiol Rev 26(2):308-341
- 394 Foster HA, Ditta IB, Varghese S, Steele A (2011) Photocatalytic disinfection using titanium dioxide:
395 spectrum and mechanism of antimicrobial activity. Appl Microbiol Biotechnol. 90(6):1847-1868
- 396 Grossweiner LI, Jones LR, Grossweiner JB, Rogers BHG (2005) Photochemical Damage to Biological
397 Systems. In *The Science of Phototherapy: an Introduction* (Ed Jones), Springer the Netherlands.
- 398 Gordon MA, Graham SM, Walsh AL, Wilson LK, Phiri A, Molyneux EM, et al. (2008) Epidemics of
399 invasive *Salmonella enterica* serovar Enteritidis and *Salmonella enterica* serovar Typhimurium
400 infection associated with multidrug resistance among adults and children in Malawi. Clin Infect Dis
401 46:963-969
- 402 Grey CE, Adlercreutz P (2003) Ability of antioxidants to prevent oxidative mutations in *Salmonella*
403 typhimurium TA102. Mutat Res 527:27–36
- 404 Haley BJ and Cole D (2009) Distribution, diversity, and seasonality of waterborne salmonellae in a
405 rural watershed. Appl Environ Microb 75(5):1248-1255
- 406 Hignen WAM and Medema GJ (2006) Inactivation credit of UV radiation for viruses, bacteria and
407 protozoan (oo)cysts in water: A review. Water Res 40(1):3-22

408 Kanno T, Nakamura K, Ikai H, Kikuchi K, Sasaki K, Niwano Y (2012) Literature review of the role of
409 hydroxyl radicals in chemically induced mutagenicity and carcinogenicity for the risk assessment of a
410 disinfection system utilizing photolysis of hydrogen peroxide. *J Clin Biochem Nutr* 51:9–14

411 Koivunen J and Heinonen-Tanski H (2005) Inactivation of enteric microorganisms with chemical
412 disinfectants, UV radiation and combined chemical/UV treatments. *Water Res* 39(8):1519-1526

413 Levantesi C, Bonadonna L, Briancesco R, Grohmann E, Toze S, Tandoi V (2012) *Salmonella* in surface
414 and drinking water: Occurrence and water-mediated transmission. *Food Res Internat* 45(2): 587-602

415 Levantesi C, La Mantia R, Masciopinto C, Uta Böckelmann C et al. (2010) Quantification of pathogenic
416 microorganisms and microbial indicators in three wastewater reclamation and managed aquifer
417 recharge facilities in Europe. *Sci Total Environ* 408(21):4923-4230

418 Li H, Bhaskara A, Megalis C, Tortorello ML (2012) Transcriptomic analysis of *Salmonella* desiccation
419 resistance. *Foodborne Pathog Dis* 9:1143–1151

420 Long M, Wang J, Zhuang H, Zhang Y, Wu H, and Zhang J (2014) Performance and mechanism of
421 standard nano-TiO₂ (P-25) in photocatalytic disinfection of foodborne microorganisms—*Salmonella*
422 typhimurium and *Listeria monocytogenes*. *Food Control* 39(1):68–74

423 Lu Z-X, Zhou L, Zhang Z-L, Shi W-L, Xie Z-X, Xie H-Y, Pang D-W, Shen P (2003) Cell Damage
424 Induced by Photocatalysis of TiO₂ Thin Films. *Langmuir* 19:8765-8768

425 Magdeburg A, Stalter D, Schlsener M, Ternes T, Oehlmann J (2014) Evaluating the efficiency of
426 advanced wastewater treatment: target analysis of organic contaminants and (geno-)toxicity assessment
427 tell a different story. *Water Res* 50(0):35-47

428 Majowicz SE, Musto J, Scallan E, Angulo FJ, Kirk M, O'Brien SJ, Jones TF, Fazil A, Hoekstra RM
429 (2010) The global burden of nontyphoidal *Salmonella gastroenteritis*. *Clin Infect Dis* 50:882–889

430 Maron DM, Ames BN (1983) Revised methods for *Salmonella* mutagenicity test. *Mutat Res* 101: 173-
431 215

432 Martinez-Urtaza J, Saco M, de Novoa J, Perez-Pineiro P, Peiteado J, Lozano-Leon A, Garcia-Martin O
433 (2004) Influence of environmental factors and human activity on the presence of *Salmonella* serovars
434 in a marine environment. *Appl Environ Microbiol* 70:2089–2097

435 Masarikova M, Manga I, Cizek A, Dolejska M, Oravcova V, Myskova P, Karpiskova R, Literak I
436 (2016) *Salmonella enterica* resistant to antimicrobials in wastewater effluents and black-headed gulls
437 in the Czech Republic, 2012. *Sci Total Environ* 542:102–107

438 McGuigan KG, Conroy RM, Mosler H-J, du Preez M, Ubomba-Jaswa E, Fernandez-Ibanez P (2012)
439 Solar water disinfection (SODIS): A review from bench-top to roof-top. J Hazard Mater 235– 236:29–
440 46

441 Michael GB, Butaye P, Cloeckaert A, Schwarz S (2006) Genes and mutations conferring antimicrobial
442 resistance in *Salmonella*: an update. Microbes Infect 8(7):1898-1914

443 Mišić M, Knasmueller S, Ferk F, Cichna-Markl M, Grummt T, Schaar H, Kreuzinger N (2011) Impact
444 of ozonation on the genotoxic activity of tertiary treated municipalwastewatr. Water Res 45(12):3681-
445 3691

446 Monarca S, Feretti D, Collivignarelli C, Guzzella G, Zerbini I, Bertanza G, Pedrazzani R (2000) The
447 influence of different disinfectants on mutagenicity and toxicity of urban wastewater. Water Res
448 34(17):4261-4269

449 Nutt JD, Li X, Woodward CL, Zabala-Diaz IB and Ricke SC (2003) Growth kinetics response of a
450 *Salmonella* Typhimurium poultry marker strain to fresh produce extracts. Bioresource Technol 89:313-
451 316

452 Oubrim N, Ennaji MM, Badri S, Cohen N (2012) Removal of Antibiotic-Resistant *Salmonella* in
453 Sewage Water from Wastewater Treatment Plants in Settat and Soualem, Morocco. Eur J Sci Res
454 68(4):565-573

455 Polo F, Figueras MJ, Inza I, Sala J, Fleisher JM, Guarro J (1999) Prevalence of *Salmonella* serotypes
456 in environmental waters and their relationships with indicator organisms. A Van Leeuw 75:285–292

457 Polo-López MI, Castro-Alfárez M, Oller I, Fernández-Ibáñez P (2014) Assessment of solar photo-
458 Fenton, photocatalysis, and H₂O₂ for removal of phytopathogen fungi spores in synthetic and real
459 effluents of urban wastewater. Chemi Eng J 257:122-130

460 Popoff M Y (2001) Antigenic formulas of the *Salmonella* serovars. WHO Collaborating Center for
461 Reference and Research on Salmonella (8th ed). Institut Pasteur Paris, France.

462 Rahmani M, Peighambari S M, Svendsen C A, Cavaco L M, Agersø Y, Hendriksen RS (2013)
463 Molecular clonality and antimicrobial resistance in *Salmonella enterica* serovars Enteritidis and Infantis
464 from broilers in three Northern regions of Iran. BMC Vet Res 9:66

465 Rahmani BA, Wasfy MO, Maksoud MA, Hanna N, Dueger E, House B (2014) Multi-drug resistance
466 and reduced susceptibility to ciprofloxacin among *Salmonella enterica* serovar Typhi isolates from the
467 Middle East and Central Asia. New Microbes and New Infect 2(4):88-92

468 Rincon AG, Pulgarin C (2007) Fe³⁺ and TiO₂ solar-light-assisted inactivation of *E. coli* at field scale
469 – implications in solar disinfection at low temperature of large quantities of water. *Catal Today* 122:
470 128–136.

471 Rizzo L (2011) Bioassays as a tool for evaluating advanced oxidation processes in water and wastewater
472 treatment. *Water Res* 45:4311-4330

473 Rizzo L, Manaia C, Merlin C, Schwartz T, Dagot C, Ploy MC, Michael I, Fatta-Kassinos D (2013)
474 Urban wastewater treatment plants as hotspots for antibiotic resistant bacteria and genes spread into the
475 environment: A review. *Sci Total Environ* 447:345-360

476 Rizzo L, Ferro G, Manaia CM (2014a) Wastewater disinfection by solar heterogeneous photocatalysis:
477 Effect on tetracycline resistant/sensitive enterococcus strains. *Global Nest Journal* 16: 455-462

478 Rizzo L, Della Sala A, Fiorentino A, Li Puma G (2014b) Disinfection of urban wastewater by solar
479 driven and UV lamp - TiO₂ photocatalysis: Effect on a multi drug resistant *Escherichia coli* strain.
480 *Water Res* 53:145-152

481 Robertson GP (2005) Functional and therapeutic significance of Akt deregulation in malignant
482 melanoma. *Cancer Metast Rev* 24:273–285

483 Sciacca J, Rengifo-Herrera J, Wethe, Pulgarin C (2011) Solar disinfection of wild *Salmonella* sp. in
484 natural water with a 18 L CPC photoreactor: Detrimental effect of non-sterile storage of treated water.
485 *Sol Energy* 85:1399–1408

486 Sharma VK, Johnson N, Cizmas L, McDonald TJ, Kim H (2016). A review of the influence of treatment
487 strategies on antibiotic resistant bacteria and antibiotic resistance genes. *Chemosphere* 150:702-714

488 Silva RC, Cardoso WM, Teixeira RSC, Albuquerque ÁH, Horn RV, Cavalcanti CM (2013) *Salmonella*
489 *Gallinarum* virulence in experimentally infected Japanese quails (*Coturnix japonica*). *Braz J of Poultr*
490 *Science* 15(1):39-45

491 Sinha RP, Häder DP (2002) UV-induced DNA damage and repair: a review. *Photochem Photobiol Sci*
492 1(4):225-236

493 Simonet J, Gantzer C (2006) Inactivation of poliovirus 1 and F-specific RNA phages and degradation
494 of their genomes by UV irradiation at 254 nanometers. *Appl Environ Microbiol* 72(12):7671-7677

495 Tate P, Stannera A, Shieldsa K, Smithc S, Larcom L (2006) Blackberry extracts inhibit UV-induced
496 mutagenesis in *Salmonella typhimurium* TA100. *Nutrition Research* 26:100–104

497 Wang J, Zhuan H, Hinton A Jr., Bowker B, Zhang J (2014) Photocatalytic disinfection of spoilage
498 bacteria *Pseudomonas fluorescens* and *Micrococcus caseolyticus* by nano-TiO₂. LWT - Food Science
499 and Technology 59(2):1009–1017

500 Wéry N, Lhoutellier C, Ducray F, Delgenès JP & Godon JJ (2008) Behaviour of Pathogenic and
501 Indicator Bacteria During Urban Wastewater Treatment and Sludge Composting, as Revealed By
502 Quantitative PCR. Water Res 42:53-62

503

504 **Figure captions**

505 **Fig. 1** Control tests on TiO₂/UV experiments: effect of UV-A radiation on the inactivation and the formation
506 of mutants for three different initial cell loads of strain TA102: 10⁹ (a), 10⁸ (b) and 10⁷ (c) CFU.mL⁻¹. Error
507 bars represent standard deviation from three independent experiments

508 **Fig. 2** Effect of TiO₂/UV process on the inactivation and the formation of mutants for three different initial
509 cell loads of strain TA102: 10⁹ (a), 10⁸ (b) and 10⁷ (c) CFU.mL⁻¹. Error bars represent standard deviation from
510 three independent experiments

511 **Fig. 3** Effect of UV-C process on the inactivation and the formation of mutants for three different initial cell
512 loads of strain TA102: 10⁹ (a), 10⁸ (b) and 10⁷ (c) CFU.mL⁻¹. Error bars represent standard deviation from
513 three independent experiments

514

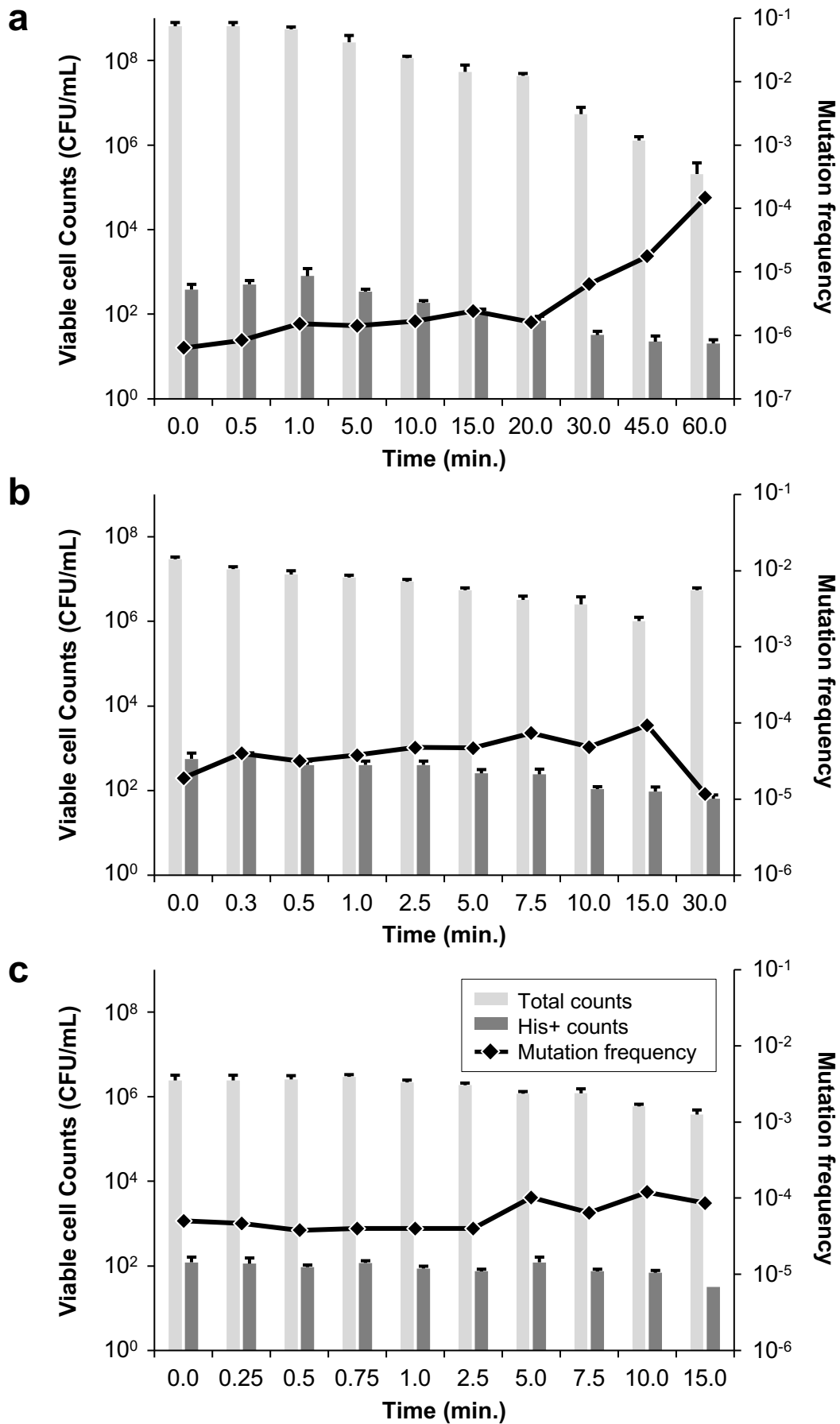


Figure 1

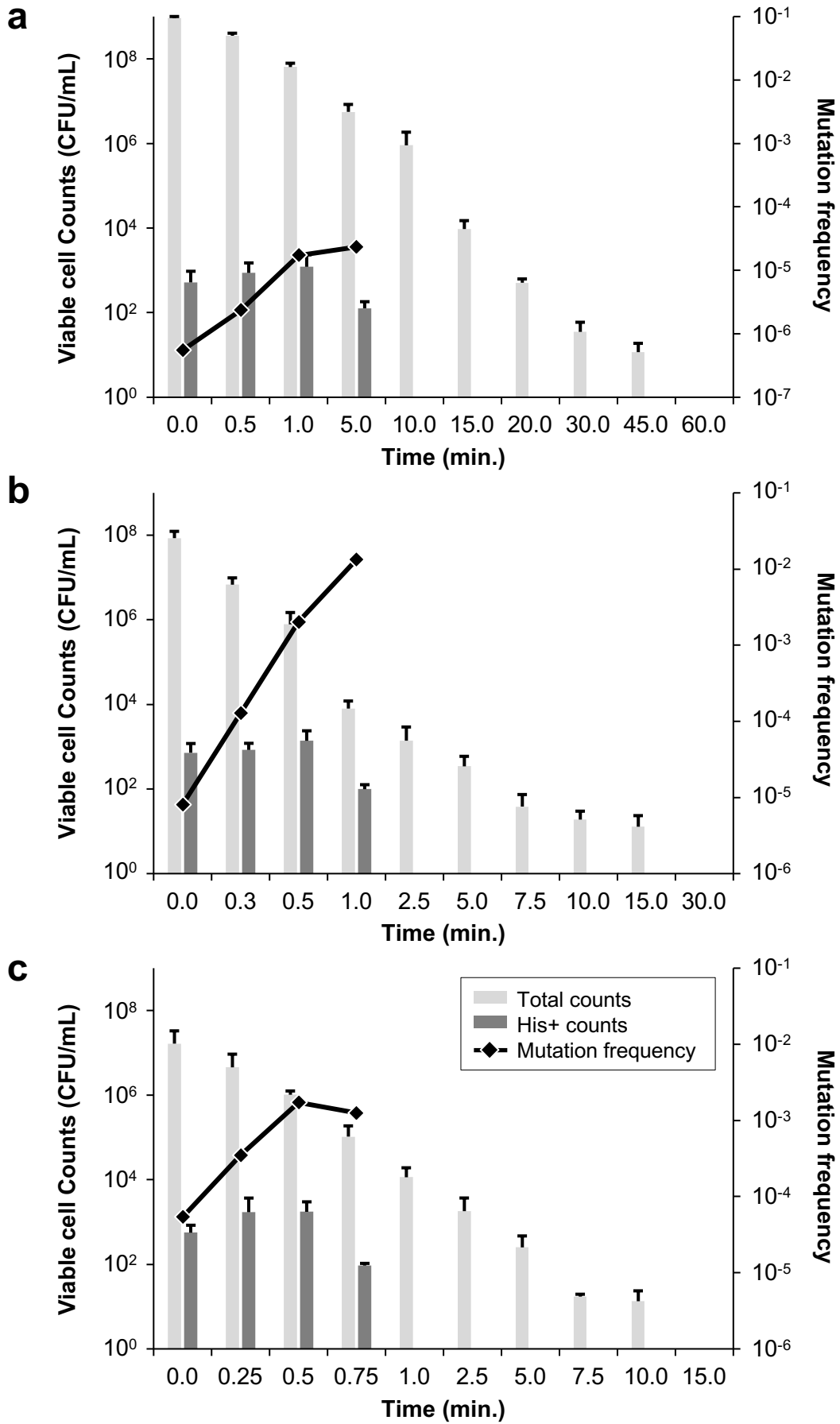


Figure 2

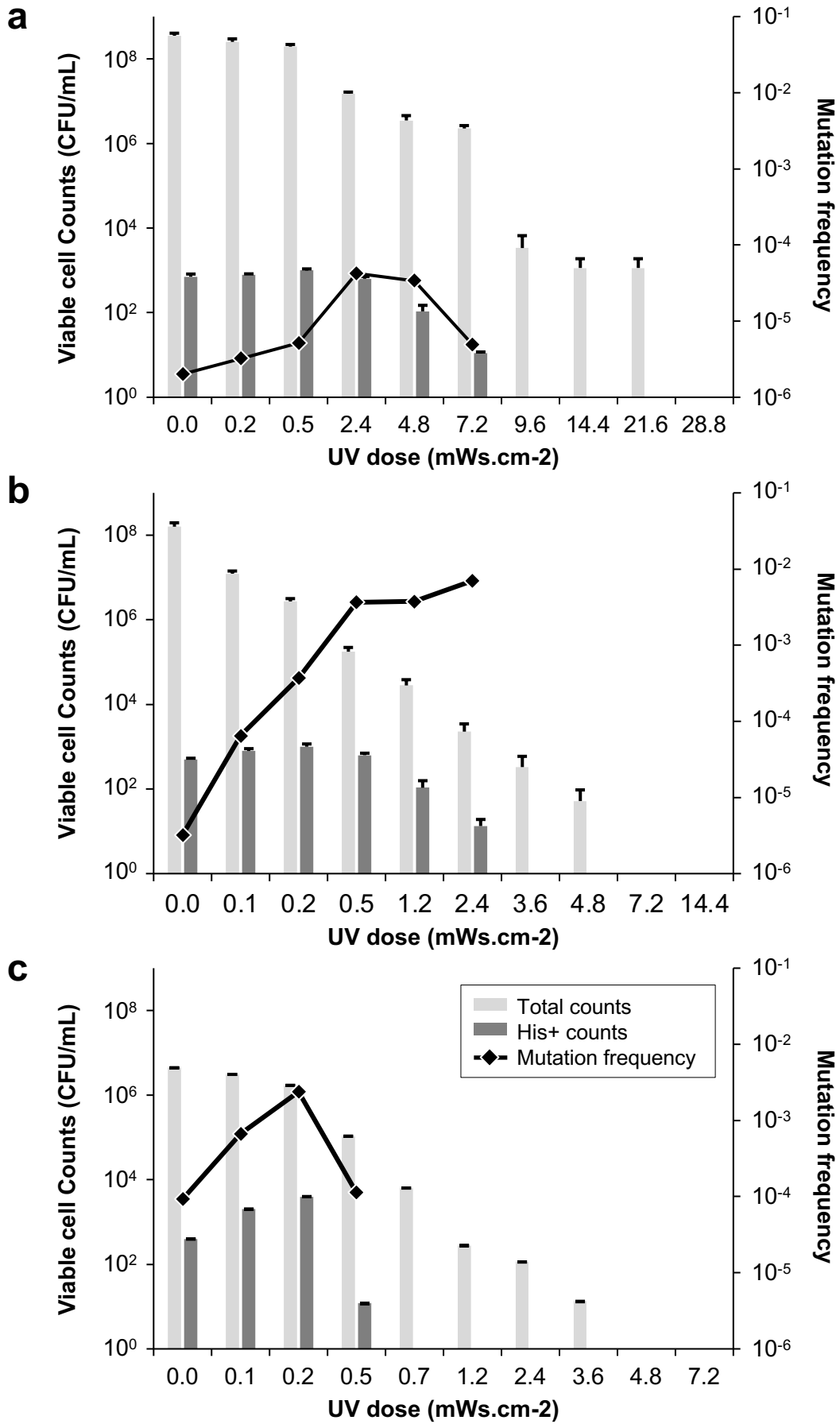


Figure 3

Supplementary material

Comparing TiO₂ photocatalysis and UV-C radiation for inactivation and mutants formation of *Salmonella typhimurium* TA102

Antonino Fiorentino, Luigi Rizzo, H el ene Guilloteau, Xavier Bellanger, Christophe Merlin.

Table of content:

1. Statistical analysis procedures
2. Dose-dependent effects of the treatments on bacterial viability
3. Statistical analysis of the UV-A treatment efficiency
 - 3.1. Regression analyses and trendline equations summaries
 - 3.2. Statistical comparison of the treatment efficiency as a function of the cell load
4. Statistical analysis of the UV-A + TiO₂ treatment efficiency
 - 4.1. Regression analyses and trendline equations summaries
 - 4.2. Statistical comparison of the treatment efficiency as a function of the cell load
5. Statistical analysis of the UV-C treatment efficiency
 - 5.1. Regression analyses and trendline equations summaries
 - 5.2. Statistical comparison of the treatment efficiency as a function of the cell load
6. Statistical comparison of the UV-A and UV-A + TiO₂ treatments

1. Statistical analysis procedures

The correlations between the bacterial mortality ($\log(N/N_0)$) and the duration of the treatments, or the doses received, were assessed using the Pearson's test. Then, regression data analyses were performed on log-transformed data: $\log(N/N_0)$ for the total cell counts and $\log(F/F_0)$ for the frequencies of mutation. The effects of both the treatment and the initial bacterial cell load were analyzed using a Fisher F-test and a Student T-test. The Fisher F-test was used to test data for homogeneity of variances. Thereafter, once homogeneity was verified, a Student T-test was further used to compare the trends (slopes) of linear regressions. A statistical difference revealed by a Student T-test, combined to the comparison of regression trend-lines (slopes) allowed determining whether a given treatment or condition had stronger effects than another one.

2. Dose-dependent effects of the treatments on bacterial viability

The dose-dependent effect of each treatment (UV-C, UV-A, and UV-A + TiO₂) on the bacterial viability (total cell count) was evaluated using a Pearson correlation test. For all conditions, the cell count abatements appeared statistically correlated to the treatment dose whatever the initial cell load (Table S1). Data were further analyzed to evaluate the statistical significance of the initial cell load and to compare treatments where possible.

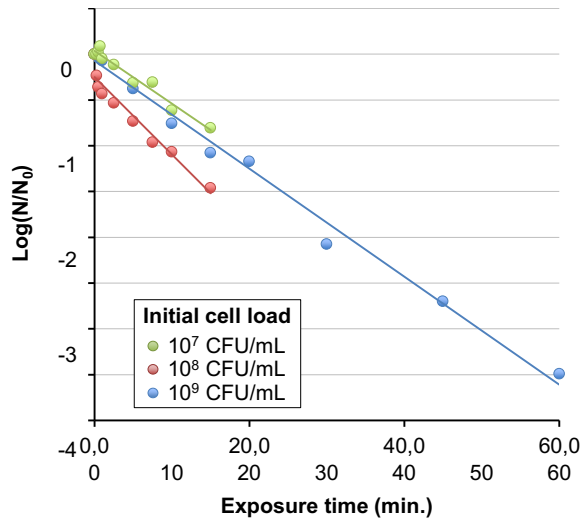
Table S1: Correlation between viable cell counts ($\log(\text{CFU/mL})$) and the treatment dose (UV-C)/treatment duration (UV-A ± TiO₂) for the three different initial cell loads. The table provides "Pearson correlation coefficient" (PCC) and p-values (between parentheses).

Initial cell loads / treatment	10 ⁹ CFU/mL	10 ⁸ CFU/mL	10 ⁷ CFU/mL
UV-C	-0.957 (1.5 × 10 ⁻⁵)	-0.840 (2.0 × 10 ⁻³)	-0.876 (8.9 × 10 ⁻⁴)
UV-A	-0.933 (7.9 × 10 ⁻⁵)	-0.750 (1.2 × 10 ⁻²)	-0.900 (3.8 × 10 ⁻⁴)
UV-A + TiO ₂	-0.988 (1.0 × 10 ⁻⁷)	-0.976 (1.3 × 10 ⁻⁶)	-0.981 (5.2 × 10 ⁻⁷)

3. Statistical analysis of the UV-A treatment efficiency

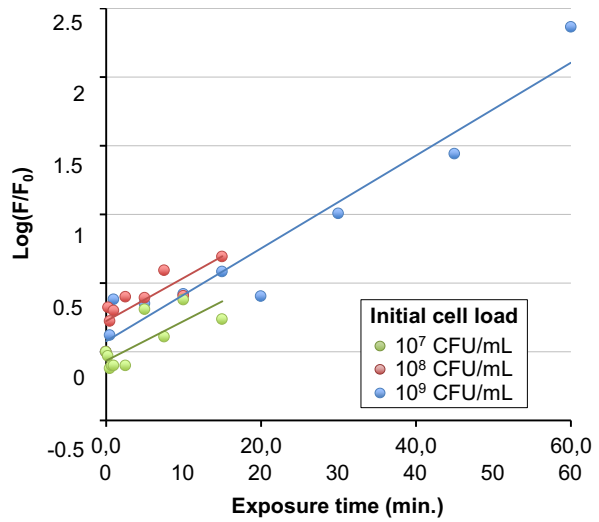
3.1. Regression analyses and trendline equations summaries

Fig. S1: Total viable cell counts abatements



Initial cell load	10 ⁹ CFU/mL	10 ⁸ CFU/mL	10 ⁷ CFU/mL
Slope	-0.059	-0.085	-0.058
r ²	0.991	0.942	0.964

Fig. S2: Evolution of mutation frequencies



Initial cell load	10 ⁹ CFU/mL	10 ⁸ CFU/mL	10 ⁷ CFU/mL
Slope	0.034	0.031	0.029
r ²	0.933	0.674	0.609

3.2. Statistical comparison of the treatment efficiency as a function of the cell load

At a first glimpse, the cell count abatement profiles (Fig. S1) and the evolution of the frequencies profiles (Fig. S2) for the UV-A treatment appeared relatively close to each other whatever the initial cell loads. This similarity was further confirmed by Student T-tests, whenever the comparison was authorized by Fisher F-tests (Tables S2 and S3).

Table S2: Comparison of total cell counts abatements for the UV-A treatment.

Initial cell load	10 ⁹ CFU/mL	10 ⁸ CFU/mL	10 ⁷ CFU/mL
10 ⁹ CFU/mL		≈	ND
10 ⁸ CFU/mL			ND
10 ⁷ CFU/mL			

Table S3: Comparison of the evolutions of mutation frequencies for the UV-A treatment.

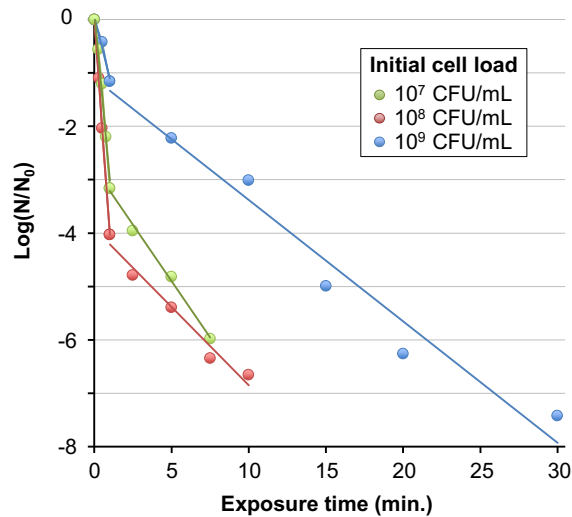
Initial cell load	10 ⁹ CFU/mL	10 ⁸ CFU/mL	10 ⁷ CFU/mL
10 ⁹ CFU/mL		≈	≈
10 ⁸ CFU/mL			≈
10 ⁷ CFU/mL			

NA : Not applicable (not enough data in the regression curve (2 points) to authorize a statistical comparison); **ND** : Not determined (variances not homogenous according to a Fisher F-test); **≠** : the trends (slopes) are significantly different ($p > 0.05$); **≈** : the trends (slopes) are statistically similar ($p \leq 0.05$).

4. Statistical analysis of the UV-A + TiO₂ treatment efficiency

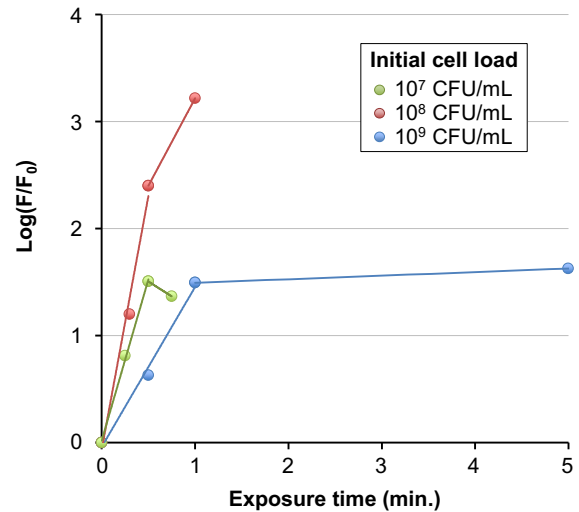
4.1. Regression analyses and trendline equations summaries

Fig. S3: Total viable cell counts abatements



Initial cell load	10 ⁹ CFU/mL		10 ⁸ CFU/mL		10 ⁷ CFU/mL	
	part 1	part 2	part 1	part 2	part 1	part 2
Curves	part 1	part 2	part 1	part 2	part 1	part 2
Slope	-1.160	-0.227	-4.062	-0.293	-3.182	-0.422
r ²	0.976	0.966	0.999	0.970	0.984	0.995

Fig. S4: Evolution of the mutation frequencies



Initial cell load	10 ⁹ CFU/mL		10 ⁸ CFU/mL		10 ⁷ CFU/mL	
	part 1	part 2	part 1	part 2	part 1	part 2
Curves	part 1	part 2	part 1	part 2	part 1	part 2
Slope	1.494	0.033	4.737	1.634	3.011	-0.553
r ²	0.992	1.000	0.987	1.000	0.998	1.000

4.2. Statistical comparison of the treatment efficiency as a function of the cell load

Both, the cell count abatement profiles (Fig. S3) and the evolution of the mutation frequencies profiles (Fig. S4) obtained for the UV-A+TiO₂ treatment tend to display a biphasic aspect with a trend linked to the initial cell loads. The biphasic aspects of the curves could be confirmed statistically by comparing the different parts of a same curve. When statistical comparisons were authorized by the Fisher F-test, the Student T-test showed that the treatment-dependent cell killing is significantly more reduced as the initial cell load increases (Fig. S3 and Table S2). Similarly, the analysis of the first part of the mutation frequency evolution curves, show that for an initial cell load of 10⁹ CFU/mL, the time-dependent increase of the mutation frequency is significantly lower than for the two other cell concentrations (Fig. S4 and Table S3).

Table S2: Comparison of total cell counts abatements for the UV-A+TiO₂ treatment.

Initial cell load / curve part	10 ⁹ CFU/mL		10 ⁸ CFU/mL		10 ⁷ CFU/mL	
	part 1	part 2	part 1	part 2	part 1	part 2
10 ⁹ CFU/mL part 1		ND	≠		≠	
10 ⁹ CFU/mL part 2			ND	≈		ND
10 ⁸ CFU/mL part 1				≠	≠	
10 ⁸ CFU/mL part 2						≠
10 ⁷ CFU/mL part 1						≠
10 ⁷ CFU/mL part 2						

Table S3: Comparison of the evolutions of mutation frequencies for the UV-A+TiO₂ treatment.

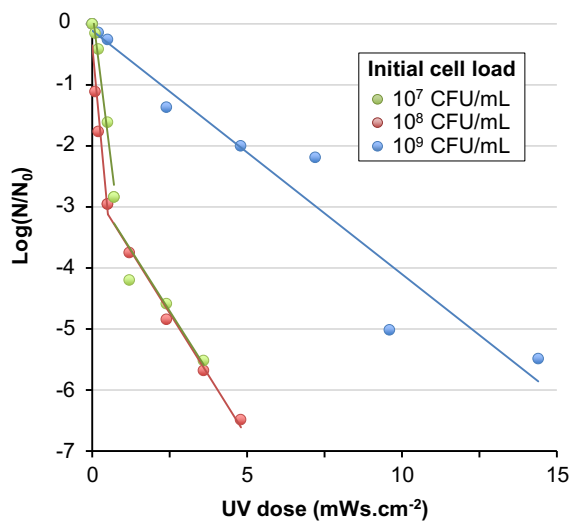
Initial cell load / curve part	10 ⁹ CFU/mL		10 ⁸ CFU/mL		10 ⁷ CFU/mL	
	part 1	part 2	part 1	part 2	part 1	part 2
10 ⁹ CFU/mL part 1		NA	≠		≠	
10 ⁹ CFU/mL part 2				NA		NA
10 ⁸ CFU/mL part 1				NA	≈	
10 ⁸ CFU/mL part 2						NA
10 ⁷ CFU/mL part 1						NA
10 ⁷ CFU/mL part 2						

NA : Not applicable (not enough data in the regression curve (2 points) to authorize a statistical comparison); **ND** : Not determined (variances not homogenous according to a Fisher F-test); **≠** : the trends (slopes) are significantly different ($p > 0.05$); **≈** : the trends (slopes) are statistically similar ($p \leq 0.05$).

5. Statistical analysis of the UV-C treatment efficiency

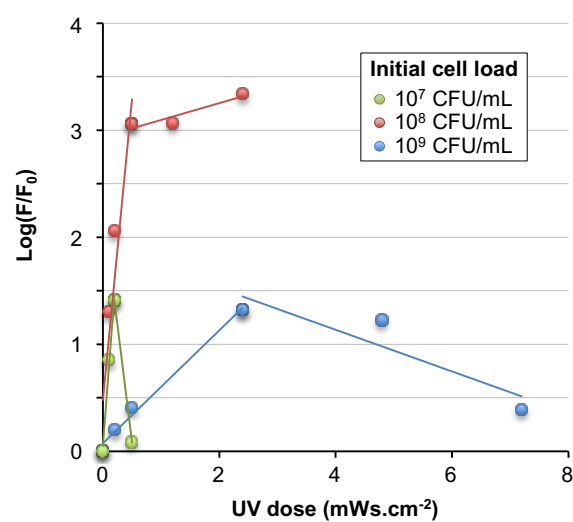
5.1. Regression analyses and trendline equations summaries

Fig. S5: Total viable cell counts abatements



Initial cell load	10 ⁹ CFU/mL		10 ⁸ CFU/mL		10 ⁷ CFU/mL	
	part 1	part 2	part 1	part 2	part 1	part 2
Curves	part 1	part 2	part 1	part 2	part 1	part 2
Slope	-0.399	-	-5.539	-0.811	-4.080	-0.800
r ²	0.937	-	0.937	0.990	0.971	0.872

Fig. S6: Evolution of the mutation frequencies



Initial cell load	10 ⁹ CFU/mL		10 ⁸ CFU/mL		10 ⁷ CFU/mL	
	part 1	part 2	part 1	part 2	part 1	part 2
Curves	part 1	part 2	part 1	part 2	part 1	part 2
Slope	0.527	-0.195	5.618	0.157	7.048	-4.419
r ²	0.989	0.828	0.887	0.888	0.985	1.000

5.2. Statistical comparison of the treatment efficiency as a function of the cell load

With the UV treatment, the biphasic aspect of the cell count abatement curves were solely observed for the initial cell loads of 10⁷ and 10⁸ CFU/mL (Fig. S5). When statistical comparison was authorized by the Fisher F-test, Student T-tests showed that for these two initial cell loads (i) the abatement curves are statistically similar and (ii) that the treatment is relatively more efficient than for an initial cell load of 10⁹ CFU/mL (Fig. S5 and Table S4). Concerning the mutation frequencies profiles, the lack

of analysable datapoints (valid Fisher tests and/or enough datapoints on the trend line) authorized comparisons in a limited number of cases, mainly the first part of the curves for the two extreme initial cell loads. In such cases the Student T-test demonstrated that mutation frequencies increased faster as the initial cell load is smaller (Fig. S6 and Table S5).

Table S4: Comparison of total cell counts abatements for the UV-C treatment.

Initial cell load / curve part		10 ⁹ CFU/mL		10 ⁸ CFU/mL		10 ⁷ CFU/mL	
		part 1		part 1	part 2	part 1	part 2
10 ⁹ CFU/mL	part 1			≠	ND	ND	≈
	part 2						
10 ⁸ CFU/mL	part 1				≠	≈	NA
	part 2					NA	≈
10 ⁷ CFU/mL	part 1						≠
	part 2						

Table S5: Comparison of the evolutions of mutation frequencies for the UV-C treatment.

Initial cell load / curve part		10 ⁹ CFU/mL		10 ⁸ CFU/mL		10 ⁷ CFU/mL	
		part 1	part 2	part 1	part 2	part 1	part 2
10 ⁹ CFU/mL	part 1		≠	ND		≠	
	part 2				≈		NA
10 ⁸ CFU/mL	part 1				≠	ND	
	part 2						NA
10 ⁷ CFU/mL	part 1						NA
	part 2						

NA : Not applicable (not enough data in the regression curve (2 points) to authorize a statistical comparison); **ND** : Not determined (variances not homogenous according to a Fisher F-test); **≠** : the trends (slopes) are significantly different ($p > 0.05$); **≈** : the trends (slopes) are statistically similar ($p \leq 0.05$).

6. Statistical comparison of the UV-A and UV-A + TiO₂ treatments

UV-A and UV-A/TiO₂ treatments, which were carried out in the same conditions, were compared using Student T-tests. Whenever it was authorized by Fisher F-tests, the comparisons of the cell count abatements showed that (i) UV-A and UV-A+TiO₂ treatments are significantly different for a given initial cell load (Table S8), and (ii) with a stronger effect of the photocatalytic treatment according to the trends (slopes) of the linear regressions (Fig. S1, Fig. S3). The same tendencies were observed for the evolution of the mutation frequencies although the statistical comparison were authorized (Fisher F-test) for the two higher initial cell loads only (Table S7, Fig. S2, Fig. S4).

Table S6: Comparison of total cell counts abatements for the UV-A and UV-A + TiO₂ treatments.

Initial cell load and treatment	10 ⁹ CFU/mL UV-A + TiO ₂		10 ⁸ CFU/mL UV-A + TiO ₂		10 ⁷ CFU/mL UV-A + TiO ₂	
	part 1	part 2	part 1	part 2	part 1	part 2
10 ⁹ CFU/mL UV-A	≠	ND				
10 ⁸ CFU/mL UV-A			≠	≠		
10 ⁷ CFU/mL UV-A					ND	≠

Table S7: Comparison of the evolutions of mutation frequencies for the UV-A and UV-A + TiO₂ treatments.

Initial cell load and treatment	10 ⁹ CFU/mL UV-A + TiO ₂	10 ⁸ CFU/mL UV-A + TiO ₂	10 ⁷ CFU/mL UV-A + TiO ₂
	part 1	part 1	part 1
10 ⁹ CFU/mL UV-A	≠		
10 ⁸ CFU/mL UV-A		≠	
10 ⁷ CFU/mL UV-A			ND

NA : Not applicable (not enough data in the regression curve (2 points) to authorize a statistical comparison); **ND** : Not determined (variances not homogenous according to a Fisher F-test); **≠** : the trends (slopes) are significantly different ($p > 0.05$); **≈** : the trends (slopes) are statistically similar ($p \leq 0.05$).